

# Gravitational decoupling, hairy black holes and conformal anomalies

Pedro Meert\*

*Center of Physics, Universidade Federal do ABC, 09210-580, Santo André, Brazil.*

Roldao da Rocha<sup>†</sup>

*Center of Mathematics, Federal University of ABC, 09210-580, Santo André, Brazil.*

Hairy black holes in the gravitational decoupling setup are studied from the perspective of conformal anomalies. Fluctuations of decoupled sources can be computed by measuring the way the trace anomaly-to-holographic Weyl anomaly ratio differs from unit. Therefore the gravitational decoupling parameter governing three hairy black hole metrics is then bounded to a range wherein one can reliably emulate AdS/CFT with gravitational decoupled solutions, in the tensor vacuum regime.

PACS numbers:

## I. INTRODUCTION

Gravitational decoupling methods comprise established successful protocols used to generate analytical solutions of the Einstein's effective field equations [1–6]. The gravitational decoupling and some extensions were studied in Refs. [7–16] and have been applied to kernel solutions of general relativity to construct new physically realistic solutions that describe stellar distributions, including anisotropic ones [17–33]. Refs. [34–36] derived accurate physical constraints on the parameters in gravitational decoupled solutions, using the WMAP, eLISA and LIGO. The gravitational decoupling procedure iteratively constructs, upon a given isotropic source of gravitational field, anisotropic compact sources of gravity, that are weakly coupled. One starts with a perfect fluid, then coupling it to more elaborated stress-energy-momentum tensors that underlie realistic compact configurations [37–57].

Any action related to a classical conformal theory is invariant under Weyl transformations. Since the variation of the action with respect to the background metric is proportional to the stress-energy-momentum tensor, then the variation of the action with respect to a conformal rescaling is proportional to the trace of the stress-energy-momentum tensor, which vanishes for conformally invariant theories. However, upon quantization, conformal invariance under Weyl rescalings may be broken and conformal anomalies set in [58]. In this case, the trace of the stress-energy-momentum tensor may achieve a non-null expectation value and, thus, a conformal anomaly regards a trace anomaly [59–64]. In the context of the gravitational decoupling procedure, comparing the holographic Weyl anomaly to the trace anomaly of the energy-momentum tensor from 4D field theory leads to a quantity that can probe and measure

the source of the gravitational decoupling [65]. Hence, the calculation of the trace anomaly-to-holographic Weyl anomaly ratio makes one capable to place the gravitational decoupling, in the context of three possible metrics describing hairy black holes, as a reliable AdS/CFT realization.

This paper is organized as follows: Sec. II is dedicated to reviewing the gravitational decoupling procedure, obtaining three different metrics for gravitational decoupled hairy black holes. In Sec. III, the trace anomalies are computed for these three solutions, from the point of view of CFT, and compared to the respective values predicted by the AdS/CFT duality. Sec. IV is dedicated to conclusions.

## II. GRAVITATIONAL DECOUPLING AND HAIRY BLACK HOLES

The gravitational decoupling procedure can be straightforwardly introduced when kernel solutions of Einstein's effective field equations can be used to decouple any intricate stress-energy-momentum tensor into manageable pieces [2, 5], including the case of hairy black holes [3]. When one regards Einstein's field equations,

$$G_{\mu\nu} := R_{\mu\nu} - \frac{1}{2}Rg_{\mu\nu} = \kappa^2 \mathring{T}_{\mu\nu}, \quad (1)$$

where the stress-energy-momentum tensor, satisfying the conservation equation  $\nabla_\mu \mathring{T}^{\mu\nu} = 0$ , can be split as

$$\mathring{T}_{\mu\nu} = \mathsf{T}_{\mu\nu} + \alpha \Theta_{\mu\nu}, \quad (2)$$

for  $\mathsf{T}_{\mu\nu}$  being a general-relativistic solution and  $\Theta_{\mu\nu}$  encoding additional sources in the gravitational sector, for  $\alpha$  being an arbitrary decoupling parameter that is not perturbative, in general. One considers static, spherically symmetric, stellar distributions described by the metric

$$ds^2 = e^{\nu(r)} dt^2 - e^{\lambda(r)} dr^2 - r^2 d\Omega^2, \quad (3)$$

\*Electronic address: [pedro.meert@ufabc.edu.br](mailto:pedro.meert@ufabc.edu.br)

†Electronic address: [roldao.rocha@ufabc.edu.br](mailto:roldao.rocha@ufabc.edu.br)

where  $d\Omega^2$  denotes the solid angle element. The Einstein's field equations (1) are equivalently written as

$$\kappa^2(\mathbb{T}_0^0 + \Theta_0^0) = \frac{1}{r^2} - e^{-\lambda} \left( \frac{1}{r^2} - \frac{\lambda'}{r} \right), \quad (4a)$$

$$\kappa^2(\mathbb{T}_1^1 + \Theta_1^1) = \frac{1}{r^2} - e^{-\lambda} \left( \frac{1}{r^2} + \frac{\nu'}{r} \right), \quad (4b)$$

$$\kappa^2(\mathbb{T}_2^2 + \Theta_2^2) = -\frac{e^{-\lambda}}{4} \left( 2\nu'' + \nu'^2 - \lambda'\nu' + 2\frac{\nu' - \lambda'}{r} \right) \quad (4c)$$

where the prime denotes the derivative with respect to the variable  $r$ . Eqs. (4a–4c) regard the effective density, and the effective radial and tangential pressures, respectively given by [2, 5]

$$\dot{\rho} = \mathbb{T}_0^0 + \Theta_0^0, \quad (5a)$$

$$\dot{p}_r = -\mathbb{T}_1^1 - \Theta_1^1, \quad (5b)$$

$$\dot{p}_t = -\mathbb{T}_2^2 - \Theta_2^2, \quad (5c)$$

with anisotropy  $\Delta = \dot{p}_t - \dot{p}_r$ . A solution to Eqs. (1) for the single kernel source  $\mathbb{T}_{\mu\nu}$  was considered [3, 5],

$$ds^2 = e^{\xi(r)} dt^2 - e^{\mu(r)} dr^2 - r^2 d\Omega^2, \quad (6)$$

where

$$e^{-\mu(r)} \equiv 1 - \frac{\kappa^2}{r} \int_0^r x^2 \mathbb{T}_0^0(x) dx = 1 - \frac{2m(r)}{r} \quad (7)$$

is the Misner–Sharp–Hernandez function. The additional source  $\Theta_{\mu\nu}$  drives the gravitational decoupling of the kernel metric (6), implemented by the mappings

$$\xi(r) \mapsto \nu(r) = \xi(r) + \alpha g(r) \quad (8a)$$

$$e^{-\mu(r)} \mapsto e^{-\lambda(r)} = e^{-\mu(r)} + \alpha f(r), \quad (8b)$$

where  $f(r)$  [ $g(r)$ ] is the geometric deformation for the radial [temporal] metric component. Eqs. (8a, 8b) split the Einstein's field equations (4a–4c) into two distinct arrays. The first one encodes the Einstein's field equations for  $\mathbb{T}_{\mu\nu}$ , solved by the kernel metric (6). The second one is associated to  $\Theta_{\mu\nu}$  and reads

$$\kappa^2 \Theta_0^0 = -\alpha \left( \frac{f}{r^2} + \frac{f'}{r} \right), \quad (9a)$$

$$\kappa^2 \Theta_1^1 + \alpha \frac{e^{-\mu} g'}{r} = -\alpha f \left( \frac{1}{r^2} + \frac{\nu'}{r} \right) \quad (9b)$$

$$\kappa^2 \Theta_2^2 + \alpha f \left( 2\nu'' + \nu'^2 + 2\frac{\nu'}{r} \right) = -\alpha \frac{f'}{4} \left( \nu' + \frac{2}{r} \right) + V, \quad (9c)$$

where  $V = \alpha e^{-\mu} \left( 2g'' + g'^2 + \frac{2g'}{r} + 2\xi' g' - \mu' g' \right)$  [1]. The tensor-vacuum, defined for  $\Theta_{\mu\nu} \neq 0$  and  $\mathbb{T}_{\mu\nu} = 0$ , leads to hairy black hole solutions [66]. Eqs. (4a, 4b) then yield a negative radial pressure,

$$\dot{p}_r = -\dot{\rho}. \quad (10)$$

and, together to the Schwarzschild solution, it implies that

$$\alpha f(r) = \left( 1 - \frac{2M}{r} \right) \left( e^{\alpha g(r)} - 1 \right), \quad (11)$$

so that the line element (3) becomes

$$ds^2 = \left( 1 - \frac{2M}{r} \right) e^{\alpha g(r)} dt^2 - \left( 1 - \frac{2M}{r} \right)^{-1} e^{-\alpha g(r)} dr^2 - r^2 d\Omega^2. \quad (12)$$

In the radial range  $r \geq 2M$ , the tensor-vacuum is assumed as  $\Theta_0^0 = a\Theta_1^1 + b\Theta_2^2$ , with  $a, b \in \mathbb{R}$ . Eqs. (9a–9c) then yield

$$br(r-2M)h'' + 2[(a+b-1)r - 2(a-1)M]h' + 2(a-1)h = 2(a-1), \quad (13)$$

for  $h(r) = e^{\alpha g(r)}$ . The solution can be written as

$$e^{\alpha g(r)} = 1 + \frac{1}{r-2M} \left[ \ell_0 + r \left( \frac{\ell}{r} \right)^n \right], \quad (14)$$

where  $\ell_0 = \alpha \ell$  is a primary hair charge, whereas  $n = 2(a-1)/b$ , with  $n > 1$  for asymptotic flatness.

This line element is produced by the effective density, the radial, and tangential pressures, respectively,

$$\dot{\rho} = \Theta_0^0 = \alpha \frac{(n-1)\ell^n}{\kappa^2 r^{n+2}}, \quad (15a)$$

$$\dot{p}_r = -\Theta_1^1 = -\dot{\rho}, \quad \dot{p}_t = -\Theta_2^2 = \frac{n}{2} \dot{\rho}. \quad (15b)$$

On the other hand, the dominant energy conditions,  $\dot{\rho} \geq |\dot{p}_r|$  and  $\dot{\rho} \geq |\dot{p}_t|$ , yield  $n \leq 2$  [2, 3, 5]. Besides, the strong energy condition,

$$\dot{\rho} + \dot{p}_r + 2\dot{p}_t \geq 0, \quad \dot{\rho} + \dot{p}_r \geq 0, \quad \dot{\rho} + \dot{p}_t \geq 0, \quad (16)$$

makes Eq. (10) to read  $\Theta_2^2 \leq 0$  and  $\Theta_0^0 \geq \Theta_2^2$ , which together with Eqs. (9a) and (9c) can be written as

$$G_1(r) := h''(r-2M) + 2h' \geq 0, \quad (17a)$$

$$G_2(r) := h''r(r-2M) + 4h'M - 2h + 2 \geq 0. \quad (17b)$$

The mapping

$$h(r) \mapsto h(r) - \frac{\ell_0}{r-2M} \quad (18)$$

leaves  $G_1(r)$  and  $G_2(r)$  invariant. Solutions with a proper horizon at  $r \sim 2M$ , which also behave approximately like the Schwarzschild metric for  $r \gg 2M$ , yield  $G_1(r) = 0$ . Hence, solving Eq. (17a) implies that

$$h(r) = c_1 - \alpha \frac{\ell - r e^{-r/M}}{r-2M}. \quad (19)$$

Also, Eq. (19) is also constrained to (17b). Replacing (19) in (12) implies the metric

$$e^\nu = e^{-\lambda} = 1 - \frac{2M}{r} + \alpha e^{-r/(\mathcal{M} - \alpha \ell/2)}, \quad (20)$$

representing a hairy black hole, where  $\mathcal{M} = M + \alpha \ell/2$ .

Now, the strong energy conditions are consistent with  $\ell \geq 2M/e^2$ , whose extremal case  $\ell = 2M/e^2$  leads to

$$e^\nu = e^{-\lambda} = 1 - \frac{2M}{r} + \alpha \left( e^{-r/M} - \frac{2M}{e^2 r} \right). \quad (21)$$

which has the horizon at  $r_{\text{HOR}} = 2M$ . The dominant energy conditions,

$$\dot{\rho} \geq |\dot{p}_r|, \quad \dot{\rho} \geq |\dot{p}_t|, \quad (22)$$

in terms of (5b) and (5c) are respectively equivalent to

$$-r(r-2M)h'' - 4(r-M)h' - 2h + 2 \geq 0, \quad (23a)$$

$$r(r-2M)h'' + 4Mh' - 2h + 2 \geq 0. \quad (23b)$$

Solving (23a) for  $r \sim 2M$  and  $r \gg M$  yields [66]

$$h(r) = 1 - \frac{1}{r-2M} \left( \alpha \ell + \alpha M e^{-r/M} - \frac{Q^2}{r} \right), \quad (24)$$

where the charge  $Q = Q(\alpha)$  encompasses also tidal charges generated by additional gravitational sectors. Eq. (24) also has to satisfy (23b), which reads

$$\frac{4Q^2}{r^2} \geq \frac{\alpha}{M} (r+2M) e^{-r/M}. \quad (25)$$

Using (24) into the line element (12), yields

$$e^\nu = e^{-\lambda} = 1 - \frac{2M + \alpha \ell}{r} + \frac{Q^2}{r^2} - \frac{\alpha M e^{-r/M}}{r}, \quad (26)$$

such that

$$\dot{\rho} = \Theta_0^0 = -\dot{p}_r = \frac{Q^2}{\kappa^2 r^4} - \frac{\alpha e^{-r/M}}{\kappa^2 r^2} \quad (27)$$

The metric (26) also represents hairy black holes, where  $Q$  and  $\ell_0 = \alpha \ell$  comprise charges generating primary hair.

The horizon radii  $r_{\text{HOR}}$  are given by solutions of

$$\alpha \ell = r_{\text{HOR}} - 2M + \frac{Q^2}{r_{\text{HOR}}} - \alpha M e^{-r_{\text{HOR}}/M}, \quad (28)$$

which allows us to write the metric functions (26) as

$$e^\nu = e^{-\lambda} = 1 - \frac{r_{\text{HOR}}}{r} \left( 1 + \frac{Q^2}{r_{\text{HOR}}^2} - \frac{\alpha M}{r_{\text{HOR}}} e^{-r_{\text{HOR}}/M} \right) + \frac{Q^2}{r^2} - \frac{\alpha M}{r} e^{-r/M}. \quad (29)$$

Evaluating the density (27) at the horizon, in addition to using the expression (28), yields

$$Q^2 \geq 4\alpha (M/e)^2 \quad \text{and} \quad \ell \geq M/e^2. \quad (30)$$

As concrete examples, one can saturate the inequalities (30), and (29) become, defining  $\mathcal{M} = M \left( 1 + \frac{\alpha}{2e^2} \right)$ ,

$$e^{\nu(\text{I})} = e^{-\lambda(\text{I})} = 1 - \frac{2M}{r} + \frac{Q^2}{r^2} - \frac{\sqrt{\alpha} Q}{2r} e^{1-2\sqrt{\alpha} r/e Q}, \quad (31)$$

which can be interpreted as a nonlinear electrodynamics coupled with gravity [3]. The event horizons are placed at  $r_{\text{HOR}} = 2M$ , and  $r_{\text{HOR}} = \frac{e}{\sqrt{\alpha}} Q$ .

In the second case, the relation

$$Q^2 = \alpha \ell M \left( 2 + \alpha e^{-\alpha \ell/M} \right), \quad (32)$$

leads to

$$e^{\nu(\text{II})} = e^{-\lambda(\text{II})} = 1 - \frac{2M + \alpha \ell}{r} + \frac{2\alpha \ell M}{r^2} - \frac{\alpha M}{r^2} e^{-r/M} \left( r - \alpha \ell e^{\frac{r-\alpha \ell}{M}} \right). \quad (33)$$

The event horizon is now at  $r_{\text{HOR}} = \alpha \ell \geq 2M$ . As  $\alpha \ell \sim M$ , Eq. (33) can be also realized as a solution in nonlinear electrodynamics coupled with gravity.

Finally, when

$$Q^2 = \alpha M (2M + \alpha \ell) e^{-\frac{(2M + \alpha \ell)}{M}}, \quad (34)$$

the metric components  $e^{\nu(\text{III})} = e^{-\lambda(\text{III})}$  read

$$e^{\nu(\text{III})} = 1 - \frac{\alpha M}{r^2} e^{-r/M} \left[ r - (2M + \alpha \ell) e^{\frac{r-(2M + \alpha \ell)}{M}} \right] - \frac{2M + \alpha \ell}{r}. \quad (35)$$

The event horizon is at  $r_{\text{HOR}} = 2M + \alpha \ell = 2\mathcal{M} \geq 2M$ .

### III. WEYL AND TRACE ANOMALIES OF GRAVITATIONAL DECOUPLED HAIRY BLACK HOLES

The holographic Weyl anomaly is reminiscent of the regularization process applied to the gravitational part of the action under conformal transformations [60]. In general, the anomaly can be expressed by

$$\mathcal{A} \propto E_{(d)} + I_{(d)}, \quad (36)$$

where  $E_{(d)}$  is the  $d$ -dimensional Euler density, and  $I_{(d)}$  denotes a conformal invariant<sup>1</sup>. In four dimensions the Euler density takes the form

$$E_{(4)} = \frac{1}{64} (K - 4R^{\mu\nu} R_{\mu\nu} + R^2). \quad (37)$$

Up to a multiplicative constant, the holographic Weyl anomaly becomes

$$\langle T \rangle_{\text{CFT}} \sim \left( R^{\mu\nu} R_{\mu\nu} - \frac{1}{3} R^2 \right). \quad (38)$$

<sup>1</sup> For  $d = 4$  this invariant is unique, being given by the contraction of the Weyl tensor to itself [60].

On the other hand, the trace anomaly is a function of the matter content on a curved background together with its geometric aspects [67]

$$\langle T \rangle_{4D} \sim (K - R^{\mu\nu} R_{\mu\nu} - \square R). \quad (39)$$

This anomaly quantifies the deviation from conformal invariance, i. e., the vanishing of this particular quantity indicates that the associated dual theory preserves conformal symmetry.

Trace anomalies from the field theory side can be compared to the one found in the CFT using the coefficient [65]

$$\Gamma = \left| 1 - \frac{\langle T \rangle_{4D}}{\langle T \rangle_{\text{CFT}}} \right|, \quad (40)$$

where the definitions given in Eqs. (38, 39) have been applied. The quantity  $K = R_{\mu\nu\rho\sigma} R^{\mu\nu\rho\sigma}$  denotes the Kretschmann scalar  $K$ . This result holds in the context of asymptotic AdS backgrounds [60] and here we discuss the possibility of emulating this result to the gravitational decoupling of hairy black holes.

The coefficient (40) can quantify how AdS/CFT is reliable in the context where the metrics (31, 33, 35) of gravitational decoupled hairy black holes are taken into account. It, in fact, measures the trace anomalies associated with them and how the additional sources back-react, in the gravitational decoupling setup. The coefficient  $\Gamma$  can formally run from 0 to infinity, and AdS/CFT can underlie this setup for values that are close to unit [65, 68]. In fact, for the Schwarzschild case,  $\langle T \rangle_{4D} \propto K$  and  $\langle T \rangle_{\text{CFT}} = 0$  yielding  $\Gamma \rightarrow \infty$ , what compromises AdS/CFT in the general-relativistic case [65].

On braneworld scenarios, one seeks for spacetimes where  $\Gamma \ll 1$ , where the quantum conformal field theory on the brane and the classical gravity on the bulk descriptions are dual and equivalent [65, 69]. The case when  $\Gamma = 1$  was obtained evaluating the coefficient (40) for a braneworld black hole solution [65]. One expects other solutions to be more intricate, as the case of gravitational decoupled hairy black holes (31, 33, 35).

In appendix A we compute explicitly the coefficient (40) for the metrics (31, 33, 35). Notice that for large values of  $r$ , all three coefficients have near unit values,

$$\lim_{r \rightarrow \infty} \Gamma^{(\text{I})} \approx 1, \quad (41)$$

$$\lim_{r \rightarrow \infty} \Gamma^{(\text{II})} \approx 1, \quad (42)$$

$$\lim_{r \rightarrow \infty} \Gamma^{(\text{III})} \approx 1. \quad (43)$$

This is interesting and relevant, as such behavior is different of the Schwarzschild kernel metric used to derive these solutions using the gravitational decoupling method. Next, the limiting expressions for  $r \rightarrow 2M$  are analyzed in Figs. 1 – 3, which display  $\Gamma|_{r \rightarrow 2M}$  as a function of  $\alpha$ . Since  $\alpha$  is not a perturbation parameter, at least technically it can assume any value. Thus the

coefficient  $\Gamma_{\text{CFT}}$  can be determined in the  $\alpha \rightarrow \infty$  limit,

$$\lim_{\substack{\alpha \rightarrow \infty \\ r \rightarrow 2M}} \Gamma^{(\text{I})} = 0.923 - \mathcal{O}\left(\frac{1}{\alpha}\right), \quad (44)$$

$$\lim_{\substack{\alpha \rightarrow \infty \\ r \rightarrow 2M}} \Gamma^{(\text{II})} = 1 + \mathcal{O}\left(\frac{1}{\alpha}\right), \quad (45)$$

$$\lim_{\substack{\alpha \rightarrow \infty \\ r \rightarrow 2M}} \Gamma^{(\text{III})} = 0. \quad (46)$$

Considering these limits along with the plots in Figs. 1 – 3, one can safely state that  $\Gamma \leq 1$  at the regions of interest, namely, for the concomitant limits  $r \rightarrow \infty$  and  $r \rightarrow 2M$ .

In Figs. 1 and 2 one can clearly see a bump, where the value of  $\Gamma$  is minimum. These values are  $\Gamma^{(\text{I})} \approx 0.367$ , when  $\alpha \approx 0.988$ , as  $\Gamma^{(\text{II})} \approx 0$ , for  $\alpha \approx 0.202$ . In fact, the tiny range  $0.2015 < \alpha < 0.2032$  yields  $\Gamma^{(\text{II})} < 3 \times 10^{-5}$ .

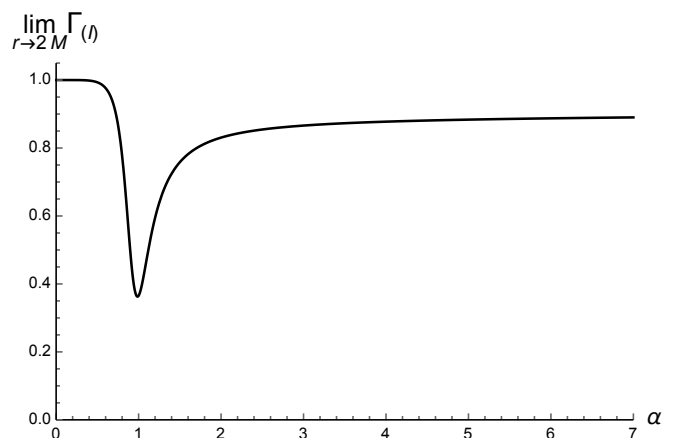


FIG. 1: Plot of  $\lim_{r \rightarrow 2M} \Gamma^{(\text{I})}$  as a function of the decoupling parameter  $\alpha$ .

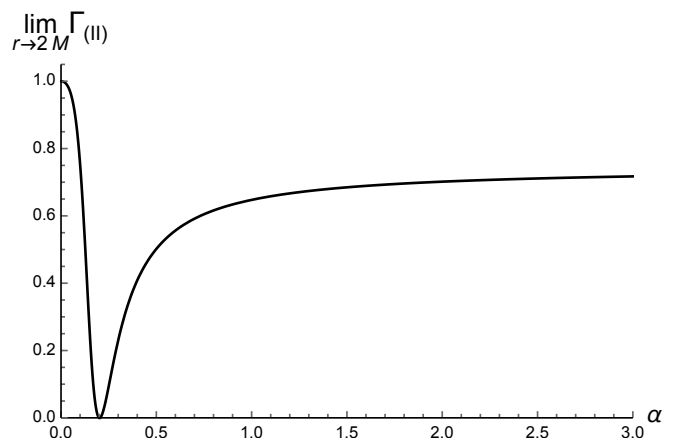


FIG. 2: Plot of  $\lim_{r \rightarrow 2M} \Gamma^{(\text{II})}$  as a function of the decoupling parameter  $\alpha$ .

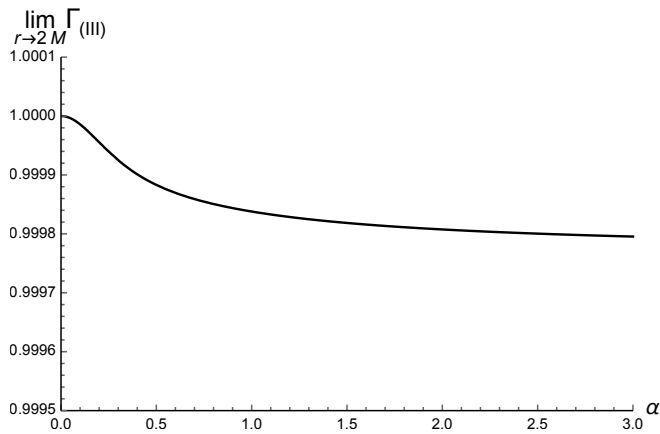


FIG. 3: Plot of  $\lim_{r \rightarrow 2M} \Gamma_{(III)}$  as a function of the decoupling parameter  $\alpha$ .

As the limiting values of  $\Gamma$  for  $r \rightarrow \infty$  do not depend on the parameter  $\alpha$ , we can use the values mentioned above on the metrics to conclude that, if the AdS/CFT correspondence holds for these particular solutions obtained via gravitational decoupling, then the best agreement between classical gravity and the associated field theory is then implemented.

#### IV. CONCLUSIONS

The gravitational decoupling of hairy black holes was utilized and inspected with the apparatus provided by trace and Weyl anomalies. The gravitational decoupling

was shown to be a trustworthy model, in the context of AdS/CFT. Since the value of the  $\Gamma$  coefficient, for the gravitational decoupling case, was shown to be near the unit, it means that the gravitational decoupling solutions may occupy a privileged place and can play a prominent role in emulating AdS/CFT on gravitational decoupled solutions. The  $\alpha \rightarrow \infty$  limit in Eqs. (44 – 46) can be seen as a regime where the stress-energy-momentum tensor (2) has only the additional source contribution, in the gravitational sector, being the general-relativistic source negligible. This characterizes, in fact, the tensor vacuum regime. The coefficient (40) quantifies the excitation of gravitationally decoupled matter fields and estimates the signatures of gravitational waves beyond the general-relativistic setup, measuring fluctuations of the decoupled source. Hence, the anomaly coefficient (40) brings useful information about placing gravitational decoupled hairy black holes in the AdS/CFT framework, implementing a method to quantify trace anomalies in this context, besides also quantifying backreaction of gravitationally decoupled additional sources, driven by the parameter  $\alpha$ .

#### Acknowledgements

This study was financed in part by the Coordenação de Aperfeiçoamento de Pessoal de Nível Superior – Brasil (CAPES) – Finance Code 001. RdR is grateful to FAPESP (Grant No. 2017/18897-8 and No. 2021/01089-1) and the National Council for Scientific and Technological Development – CNPq (Grants No. 303390/2019-0 and No. 406134/2018-9), for partial financial support.

#### Appendix A

For the first hairy black hole metric (31), one can compute the anomalies, as well as the  $\Gamma$  coefficient, as

$$\begin{aligned}
 \langle T_{(I)} \rangle_{\text{CFT}} &= \frac{2\alpha^2 e^{2 - \frac{4\sqrt{\alpha}r}{eQ}}}{3e^4 Q^2 r^4} (e^2 Q^2 + 4\sqrt{\alpha}eQr + \alpha r^2) - \frac{4\alpha Q e^{1 - \frac{2\sqrt{\alpha}r}{eQ}}}{e^2 r^6} (eQ + \sqrt{\alpha}r) + \frac{4Q^4}{r^8}, \\
 \langle T_{(I)} \rangle_{4D} &= \frac{e^{-\frac{4\sqrt{\alpha}r}{eQ}}}{e^4 Q^3 r^8} \left\{ e^4 Q^3 (48M^2 r^2 - 96MQ^2 r + 52Q^4) e^{\frac{4\sqrt{\alpha}r}{eQ}} + e\alpha^{3/2} e^2 Q^2 r^3 \left[ e\sqrt{\alpha}Qr - 4(r(M - 2r) + 2Q^2) e^{\frac{2\sqrt{\alpha}r}{eQ}} \right] \right. \\
 &\quad + 2e\alpha^{5/2} r^5 \left[ 5e\sqrt{\alpha}Qr - 4(Q^2 - 2Mr + r^2) e^{\frac{2\sqrt{\alpha}r}{eQ}} \right] + 4e\alpha^2 eQr^5 \left( 2(r - M) e^{\frac{2\sqrt{\alpha}r}{eQ}} + e\sqrt{\alpha}Q \right) \\
 &\quad \left. - 24\sqrt{\alpha}Qr (Q^2 - Mr) e^{\frac{2\sqrt{\alpha}r}{eQ} + 1} + 4e\alpha^3 Q^3 r^2 \left[ (4Mr - 6Q^2 + r^2) e^{\frac{2\sqrt{\alpha}r}{eQ}} + e\sqrt{\alpha}Qr \right] \right\}.
 \end{aligned} \tag{A1}$$

Consequently,

$$\Gamma_{(I)} = \frac{A(r, \alpha, Q)}{B(r, \alpha, Q)}, \tag{A3}$$

where

$$A(r, \alpha, Q) = e\alpha^{3/2}e^2Q^2r^3 \left[ e\sqrt{\alpha}Qr - 12[r(M-2r)+Q^2]e^{\frac{2\sqrt{\alpha}r}{eQ}} \right] + 12e\alpha e^3Q^3r^2 \left[ (4Mr-5Q^2+r^2)e^{\frac{2\sqrt{\alpha}r}{eQ}} + e\sqrt{\alpha}Qr \right] \\ + 9e^4Q^3 \left[ e\sqrt{\alpha}Qr - 4[Q^2-Mr]e^{\frac{2\sqrt{\alpha}r}{eQ}} \right]^2 + 4e\alpha^{5/2}r^5 \left[ 7e\sqrt{\alpha}Qr - 6(-2Mr+Q^2+r^2)e^{\frac{2\sqrt{\alpha}r}{eQ}} \right] \\ + 4e\alpha^2eQr^5 \left( 6(r-M)e^{\frac{2\sqrt{\alpha}r}{eQ}} + e\sqrt{\alpha}Q \right), \quad (\text{A4})$$

$$B(r, \alpha, Q) = 3 \left[ 4e^4Q^3(12M^2r^2-24MQ^2r+13Q^4)e^{\frac{4\sqrt{\alpha}r}{eQ}} - 4\sqrt{\alpha}re^{\frac{2\sqrt{\alpha}r}{eQ}+1}(\alpha e^2Q^2r^2(r(M-2r)+2Q^2)) \right. \\ \left. + \sqrt{\alpha}e^3Q^3r(6Q^2-r(4M+r))+6e^4(Q^6-MQ^4r)+2\alpha^{3/2}eQr^4(M-r)+2\alpha^2r^4(r(r-2M)+Q^2)) \right. \\ \left. + e^2\alpha Qr^2(\alpha e^2Q^2r^2+4\sqrt{\alpha}e^3Q^3r+3e^4Q^4+4\alpha^{3/2}eQr^3+10\alpha^2r^4) \right]. \quad (\text{A5})$$

The anomalies for the second hairy black hole metric (33) are respectively given by

$$\langle \mathbb{T}_{(\text{II})} \rangle_{\text{CFT}} = \frac{\alpha^2 e^{-\frac{2(\alpha\ell+r)}{M}}}{6M^2r^8} \left( 24\ell^2 M^4 e^{\frac{2r}{M}} \left( \alpha+2e^{\frac{\alpha\ell}{M}} \right)^2 - 12\ell M^2 r^2 (2M+r) \left( \alpha+2e^{\frac{\alpha\ell}{M}} \right) e^{\frac{\alpha\ell+r}{M}} + r^4 (4M^2+8Mr+r^2) e^{\frac{2\alpha\ell}{M}} \right), \quad (\text{A6})$$

$$\langle \mathbb{T}_{(\text{II})} \rangle_{4\text{D}} = \frac{e^{-\frac{2(\alpha\ell+r)}{M}}}{2M^3r^8} \left\{ 8M^3 e^{\frac{2(\alpha\ell+r)}{M}} \left( \alpha^2 \ell^2 (52M^2-24Mr+3r^2) + 12\alpha\ell Mr(r-4M) + 12M^2 r^2 \right) + 104\alpha^4 \ell^2 M^5 e^{\frac{2r}{M}} \right. \\ \left. - 2\alpha^3 \ell Mr (4M^2 r^2 + 24M^3 r + 48M^4 + r^4) e^{\frac{\alpha\ell+r}{M}} + \alpha^2 Mr^2 (2M^2 r^2 + 16M^3 r + 24M^4 + 4Mr^3 + 5r^4) e^{\frac{2\alpha\ell}{M}} \right. \\ \left. - 48M^5 (r-2\alpha) + 8M^4 r (3\alpha\ell-2r) + Mr^4 (3\alpha\ell-4r) + r^5 (r-\alpha) - 2M^3 r^3 \right. \\ \left. + 32\alpha^2 \ell M^4 e^{\frac{\alpha\ell+2r}{M}} (13\alpha\ell M - 3\alpha\ell r - 6Mr) \right\}. \quad (\text{A7})$$

Consequently,

$$\Gamma_{(\text{II})} = 1 - \frac{C(r, \alpha, Q)}{D(r, \alpha, Q)}, \quad (\text{A8})$$

where

$$C(r, \alpha, Q) = \alpha^2 M \left[ 24\ell^2 M^4 e^{\frac{2r}{M}} \left( \alpha+2e^{\frac{\alpha\ell}{M}} \right)^2 - 12\ell M^2 r^2 (2M+r) \left( \alpha+2e^{\frac{\alpha\ell}{M}} \right) e^{\frac{\alpha\ell+r}{M}} + r^4 (4M^2+8Mr+r^2) e^{\frac{2\alpha\ell}{M}} \right], \quad (\text{A9})$$

$$D(r, \alpha, Q) = 3 \left[ 8M^3 e^{\frac{2(\alpha\ell+r)}{M}} \left( \alpha^2 \ell^2 (52M^2-24Mr+3r^2) + 12\alpha\ell Mr(r-4M) + 12M^2 r^2 \right) + 104\alpha^4 \ell^2 M^5 e^{\frac{2r}{M}} \right. \\ \left. - 2\alpha^3 \ell Mr (4M^2 r^2 + 24M^3 r + 48M^4 + r^4) e^{\frac{\alpha\ell+r}{M}} + \alpha^2 Mr^2 (2M^2 r^2 + 16M^3 r + 24M^4 + 4Mr^3 + 5r^4) e^{\frac{2\alpha\ell}{M}} \right. \\ \left. - 2\alpha r e^{\frac{2\alpha\ell+r}{M}} (M^2 r^3 (\alpha-2r) - 48M^5 (r-2\alpha) + 8M^4 r (3\alpha\ell-2r) + Mr^4 (3\alpha\ell-4r) + r^5 (r-\alpha) - 2M^3 r^3) \right. \\ \left. + 32\alpha^2 \ell M^4 e^{\frac{\alpha\ell+2r}{M}} (13\alpha\ell M - 3\alpha\ell r - 6Mr) \right]. \quad (\text{A10})$$

Besides, the anomalies for the third hairy black hole metric (35) read

$$\langle \mathbb{T}_{(\text{III})} \rangle_{\text{CFT}} = \frac{\alpha^2}{6r^8} \left( 24M^2 e^{-\frac{2\alpha\ell}{M}-4} (\alpha\ell+2M)^2 - 12r^2 (2M+r) (\alpha\ell+2M) e^{-\frac{\alpha\ell+2M+r}{M}} + \frac{r^4 e^{-\frac{2r}{M}} (4M^2+8Mr+r^2)}{M^2} \right) \quad (\text{A11})$$

$$\langle \mathbb{T}_{(\text{III})} \rangle_{4\text{D}} = \frac{e^{-\frac{2(\alpha\ell+2M+r)}{M}}}{2M^3r^8} \left\{ \alpha^2 Mr^2 (2M^2 r^2 + 16M^3 r + 24M^4 + 4Mr^3 + 5r^4) e^{\frac{2\alpha\ell}{M}+4} \right. \\ \left. - 2\alpha^2 Mr (4M^2 r^2 + 24M^3 r + 48M^4 + r^4) (\alpha\ell+2M) e^{\frac{\alpha\ell+2M+r}{M}} + 24M^3 r^2 (\alpha\ell+2M)^2 e^{\frac{2(\alpha\ell+2M+r)}{M}} \right. \\ \left. + 2\alpha r^2 e^{\frac{2\alpha\ell+4M+r}{M}} (M^2 r^2 (2r-\alpha) + 8M^4 (3\alpha\ell+2r) + 2M^3 r (4\alpha\ell+r) + Mr^3 (4r-\alpha)) \right. \\ \left. + r^4 (\alpha\ell-r) + 48M^5 + 104\alpha^2 M^5 e^{\frac{2r}{M}} (\alpha\ell+2M)^2 - 96\alpha M^4 r (\alpha\ell+2M)^2 e^{\frac{\alpha\ell+2(M+r)}{M}} \right\} \quad (\text{A12})$$

$$\Gamma_{(\text{III})} = \frac{p(r, \alpha, Q)}{q(r, \alpha, Q)} \quad (\text{A13})$$



where the coefficient functions in Eq. (A13) are respectively given by

$$p(r, \alpha, Q) = 2M^3 r^8 e^{\frac{2(\alpha\ell+2M+r)}{M}} \frac{h(r, \alpha, Q)}{k(r, \alpha, Q)}, \quad (\text{A14})$$

for

$$h(r, \alpha, Q) = e^{-\frac{2(\alpha\ell+2M+r)}{M}} \left[ \alpha^2 M r^2 (2M^2 r^2 + 16M^3 r + 24M^4 + 4M r^3 + 5r^4) e^{\frac{2\alpha\ell}{M} + 4} + 24M^3 r^2 (\alpha\ell + 2M)^2 e^{\frac{2(\alpha\ell+2M+r)}{M}} + \right. \\ \left. - 2\alpha^2 M r (4M^2 r^2 + 24M^3 r + 48M^4 + r^4) (\alpha\ell + 2M) e^{\frac{\alpha\ell+2M+r}{M}} + 104\alpha^2 M^5 e^{\frac{2r}{M}} (\alpha\ell + 2M)^2 \right. \\ \left. + 2\alpha r^2 e^{\frac{2\alpha\ell+4M+r}{M}} (M^2 r^2 (2r - \alpha\ell) + 8M^4 (3\alpha\ell + 2r) + 2M^3 r (4\alpha\ell + r) + M r^3 (4r - \alpha\ell) + r^4 (\alpha\ell - r) + 48M^5) \right. \\ \left. - 96\alpha M^4 r (\alpha\ell + 2M)^2 e^{\frac{\alpha\ell+2(M+r)}{M}} \right], \quad (\text{A15})$$

$$k(r, \alpha, Q) = 2M^3 r^8 - \frac{\alpha^2}{6r^8} \left[ 24M^2 e^{-\frac{2\alpha\ell}{M} - 4} (\alpha\ell + 2M)^2 - 12r^2 (\alpha\ell + 2M) e^{-\frac{\alpha\ell+2M+r}{M}} + \frac{r^4}{M^2} e^{-\frac{2r}{M}} (4M^2 + 8Mr + r^2) \right], \quad (\text{A16})$$

and

$$q(r, \alpha, Q) = \alpha^2 M r^2 (2M^2 r^2 + 16M^3 r + 24M^4 + 4M r^3 + 5r^4) - 2\alpha^2 M r (4M^2 r^2 + 24M^3 r + 48M^4 + r^4) (\alpha\ell + 2M) e^{\frac{\alpha\ell+2M+r}{M}} \\ + 2\alpha r^2 e^{\frac{2\alpha\ell+4M+r}{M}} (M^2 r^2 (2r - \alpha\ell) + 8M^4 (3\alpha\ell + 2r) + 2M^3 r (4\alpha\ell + r) + M r^3 (4r - \alpha\ell) + r^4 (\alpha\ell - r) + 48M^5) \\ + 24M^3 r^2 (\alpha\ell + 2M)^2 e^{\frac{2(\alpha\ell+2M+r)}{M}} + 104\alpha^2 M^5 e^{\frac{2r}{M}} (\alpha\ell + 2M)^2 - 96\alpha M^4 r (\alpha\ell + 2M)^2 e^{\frac{\alpha\ell+2(M+r)}{M}}. \quad (\text{A17})$$

- 
- [1] Ovalle J 2017 *Phys. Rev.* **D95** 104019 (*Preprint* 1704.05899)
- [2] Ovalle J 2019 *Phys. Lett.* **B788** 213–218 (*Preprint* 1812.03000)
- [3] Ovalle J, Casadio R, Contreras E and Sotomayor A 2021 *Phys. Dark Univ.* **31** 100744 (*Preprint* 2006.06735)
- [4] Casadio R and Ovalle J 2014 *Gen. Rel. Grav.* **46** 1669 (*Preprint* 1212.0409)
- [5] Ovalle J, Casadio R, da Rocha R and Sotomayor A 2018 *Eur. Phys. J.* **C78** 122 (*Preprint* 1708.00407)
- [6] Antoniadis I, Arkani-Hamed N, Dimopoulos S and Dvali G R 1998 *Phys. Lett.* **B436** 257 (*Preprint* 9804398)
- [7] Casadio R and Ovalle J 2014 *Gen. Rel. Grav.* **46** 1669 (*Preprint* 1212.0409)
- [8] Ovalle J, Gergely L A and Casadio R 2015 *Class. Quant. Grav.* **32** 045015 (*Preprint* 1405.0252)
- [9] Ovalle J, Casadio R and Sotomayor A 2017 *Adv. High Energy Phys.* **2017** 9756914 (*Preprint* 1612.07926)
- [10] Casadio R, Ovalle J and da Rocha R 2014 *Class. Quant. Grav.* **31** 045016 (*Preprint* 1310.5853)
- [11] Ovalle J, Linares F, Pasqua A and Sotomayor A 2013 *Class. Quant. Grav.* **30** 175019 (*Preprint* 1304.5995)
- [12] Ovalle J and Linares F 2013 *Phys. Rev.* **D88** 104026 (*Preprint* 1311.1844)
- [13] Ovalle J and Sotomayor A 2018 *Eur. Phys. J. Plus* **133** 428 (*Preprint* 1811.01300)
- [14] Casadio R and Ovalle J 2012 *Phys. Lett.* **B715** 251–255 (*Preprint* 1201.6145)
- [15] Casadio R, Ovalle J and da Rocha R 2015 *EPL* **110** 40003 (*Preprint* 1503.02316)
- [16] Casadio R and da Rocha R 2016 *Phys. Lett.* **B763** 434–438 (*Preprint* 1610.01572)
- [17] da Rocha R 2020 *Symmetry* **12** 508 (*Preprint* 2002.10972)
- [18] Fernandes-Silva A and da Rocha R 2018 *Eur. Phys. J.* **C78** 271 (*Preprint* 1708.08686)
- [19] Contreras E 2018 *Eur. Phys. J.* **C78** 678 (*Preprint* 1807.03252)
- [20] Ovalle J 2008 *Mod. Phys. Lett.* **A23** 3247–3263 (*Preprint* gr-qc/0703095)
- [21] Sharif M and Saba S 2018 *Eur. Phys. J.* **C78** 921 (*Preprint* 1811.08112)
- [22] Sharif M and Sadiq S 2019 *Chin. J. Phys.* **60** 279–289
- [23] Morales E and Tello-Ortiz F 2018 *Eur. Phys. J.* **C78** 841 (*Preprint* 1808.01699)
- [24] Rincón A, Gabbanelli L, Contreras E and Tello-Ortiz F 2019 *Eur. Phys. J. C* **79** 873 (*Preprint* 1909.00500)
- [25] Hensh S and Stuchlik Z 2019 *Eur. Phys. J. C* **79** 834 (*Preprint* 1906.08368)
- [26] Ovalle J, Posada C and Stuchlik Z 2019 *Class. Quant. Grav.* **36** 205010 (*Preprint* 1905.12452)
- [27] Gabbanelli L, Ovalle J, Sotomayor A, Stuchlik Z and Casadio R 2019 *Eur. Phys. J. C* **79** 486 (*Preprint* 1905.10162)
- [28] Tello-Ortiz F 2020 *Eur. Phys. J.* **C80** 413
- [29] Gabbanelli L, Rincón A and Rubio C 2018 *Eur. Phys. J.* **C78** 370 (*Preprint* 1802.08000)
- [30] Panotopoulos G and Rincón A 2018 *Eur. Phys. J.* **C78** 851 (*Preprint* 1810.08830)
- [31] Heras C L and Leon P 2018 *Fortsch. Phys.* **66** 1800036 (*Preprint* 1804.06874)
- [32] Contreras E and Bargeño P 2018 *Eur. Phys. J.* **C78** 558 (*Preprint* 1805.10565)
- [33] Tello-Ortiz F, Maurya S and Gomez-Leyton Y 2020 *Eur.*

- Phys. J. C* **80** 324
- [34] Fernandes-Silva A, Ferreira-Martins A J and da Rocha R 2019 *Phys. Lett.* **B791** 323–330 (*Preprint* 1901.07492)
- [35] da Rocha R 2017 *Phys. Rev.* **D95** 124017 (*Preprint* 1701.00761)
- [36] Fernandes-Silva A, Ferreira-Martins A J and da Rocha R 2018 *Eur. Phys. J.* **C78** 631 (*Preprint* 1803.03336)
- [37] Maurya S, Maharaj S and Deb D 2019 *Eur. Phys. J. C* **79** 170
- [38] Pérez Graterol R 2018 *Eur. Phys. J. Plus* **133** 244
- [39] Morales E and Tello-Ortiz F 2018 *Eur. Phys. J.* **C78** 618 (*Preprint* 1805.00592)
- [40] Contreras E, Rincón A and Bargueño P 2019 *Eur. Phys. J.* **C79** 216 (*Preprint* 1902.02033)
- [41] Contreras E 2019 *Class. Quant. Grav.* **36** 095004 (*Preprint* 1901.00231)
- [42] Singh K, Maurya S, Jasim M and Rahaman F 2019 *Eur. Phys. J. C* **79** 851
- [43] Tello-Ortiz F, Maurya S K, Errehymy A, Singh K and Daoud M 2019 *Eur. Phys. J.* **C79** 885
- [44] Maurya S and Tello-Ortiz F 2020 *Phys. Dark Univ.* **29** 100577 (*Preprint* 1907.13456)
- [45] Linares Cedeno F X and Contreras E 2020 *Phys. Dark Univ.* **28** 100543 (*Preprint* 1907.04892)
- [46] Sharif M and Sadiq S 2018 *Eur. Phys. J.* **C78** 410 (*Preprint* 1804.09616)
- [47] Estrada M and Tello-Ortiz F 2018 *Eur. Phys. J. Plus* **133** 453 (*Preprint* 1803.02344)
- [48] Torres-Sanchez V and Contreras E 2019 *Eur. Phys. J. C* **79** 829 (*Preprint* 1908.08194)
- [49] Abellán G, Rincon A, Fuenmayor E and Contreras E 2020 (*Preprint* 2001.07961)
- [50] Estrada M and Prado R 2019 *Eur. Phys. J. Plus* **134** 168 (*Preprint* 1809.03591)
- [51] León P and Sotomayor A 2019 *Fortsch. Phys.* **67** 1900077 (*Preprint* 1907.11763)
- [52] Casadio R, Contreras E, Ovalle J, Sotomayor A and Stuchlick Z 2019 *Eur. Phys. J. C* **79** 826 (*Preprint* 1909.01902)
- [53] Sharif M and Waseem A 2019 *Annals Phys.* **405** 14–28
- [54] Abellan G, Torres-Sanchez V, Fuenmayor E and Contreras E 2020 *Eur. Phys. J. C* **80** 177 (*Preprint* 2001.08573)
- [55] Rincón A, Contreras E, Tello-Ortiz F, Bargueno P and Abellán G 2020 *Eur. Phys. J. C* **80** 490 (*Preprint* 2005.10991)
- [56] Sharif M and Majid A 2020 *Phys. Dark Univ.* **30** 100610 (*Preprint* 2006.04578)
- [57] Maurya S, Singh K N and Dayanandan B 2020 *Eur. Phys. J. C* **80** 448
- [58] Capper D and Duff M 1974 *Nucl. Phys. B* **82** 147
- [59] Duff M 1994 *Class. Quant. Grav.* **11** 1387–1404 (*Preprint* hep-th/9308075)
- [60] Henningson M and Skenderis K 1998 *JHEP* **07** 023 (*Preprint* hep-th/9806087)
- [61] Kuntz I 2018 *Eur. Phys. J. C* **78** 3 (*Preprint* 1712.06582)
- [62] Bonora L, Cotta-Ramusino P and Reina C 1983 *Phys. Lett. B* **126** 305–308
- [63] Bonora L, Giaccari S and Lima de Souza B 2014 *JHEP* **07** 117 (*Preprint* 1403.2606)
- [64] Kuntz I and da Rocha R 2020 *Nucl. Phys. B* **961** 115265 (*Preprint* 1909.10121)
- [65] Casadio R 2004 *Phys. Rev. D* **69** 084025 (*Preprint* hep-th/0302171)
- [66] Ovalle J, Casadio R, da Rocha R, Sotomayor A and Stuchlick Z 2018 *Eur. Phys. J.* **C78** 960 (*Preprint* 1804.03468)
- [67] Birrell N and Davies P 1984 *Quantum Fields in Curved Space* Cambridge Monographs on Mathematical Physics (Cambridge, UK: Cambridge Univ. Press) ISBN 978-0-521-27858-4, 978-0-521-27858-4
- [68] Meert P and da Rocha R 2021 *Nucl. Phys. B* **967** 115420 (*Preprint* 2006.02564)
- [69] Shiromizu T, Torii T and Ida D 2002 *JHEP* **03** 007 (*Preprint* hep-th/0105256)